

Multiple-Channel Scattering Resonance of One-Dimensional Ultracold Spinor Bosons

Xiaoling Cui

Beijing National Laboratory for Condensed Matter Physics,
Institute of Physics, Chinese Academy of Sciences, Beijing 100190, China

(Dated: September 2, 2014)

So far the interaction of ultracold atoms can only be tuned within one particular scattering channel near a resonance, where the spinor structure of atomic isotopes is destroyed due to the typically large magnetic field. In this work, we propose a scheme to realize *multiple-channel scattering resonance* (MCSR) of ultracold bosons in one-dimension while still keeping their spinor structure. The MCSR refers to a simultaneous scattering resonance among all different scattering channels, including those breaking SU(2) and SO(2) spin rotation symmetries. Essential ingredients for MCSR include the 3D interactions, the confinement potential and a spin-flipping field. Near MCSR a many-body spinor system exhibits exotic spin density distributions and pair correlations, which are significantly different from those near a single-channel resonance.

I. INTRODUCTION

Easy access to strong coupling regime of interacting particles and full liberation of the bosonic and fermionic spin degree of freedom comprise two unique and important features of ultracold atomic gases. Especially, the former allows the exploration of intriguing properties of strongly correlated many-body systems, such as the BCS-BEC crossover, the universal thermodynamics, and the Tonks and super-Tonks continuity of one-dimensional(1D) gas[1–3]. For the latter, taking advantage of the high (hyperfine) spin structure of atomic isotopes and the SU(2)-invariant interaction at low fields, the atomic spinor system has been shown to exhibit diverse spin textures in the ground state[4–8], and interestingly coherent spin-exchange dynamics[9–14].

Despite all these achievements, little attention has been paid to spinor system with strong interactions[15]. An essential reason is this requires the combination of both accessing to strong coupling regime and keeping the spinor structure unchanged, which are hard to realize simultaneously in the experiments so far. Specifically, the widely used approaches to strong couplings involve the techniques of Feshbach resonance(FR) in 3D[16] and the confinement-induced-resonance(CIR) in low-D[17–21]. Both of them can only tune the interaction in one particular spin-collision channel, but not the others, near a selected resonance[16, 19–21]. The residue symmetry is thus SO(2) symmetry with only the total magnetization conserved but not the total spin anymore. Even worse, near these resonances the magnetic field is typically as large as hundreds of Gauss, where the system tends to be fully polarized by the large Zeeman splitting and thus loses the spinor structure (which requires Zeeman splitting much smaller than interaction energy[4]).

In this work, we aim at generating strong coupling in multiple scattering channels with the spinor structure still maintained. Specifically, we propose a two-species bosonic spinor system in 1D geometry with strong interactions. Here the advantage of 1D geometry is that the atom loss is strongly suppressed at strong couplings[22], in contrary to the 3D counterpart. To realize such a sys-

tem, we apply a radio-frequency(rf) field and an external magnetic field, which respectively induces spin flips and tunes the interaction in a single scattering channel. We show that this system exhibits new physics incorporating both features of multiple-spin degree of freedom and strong coupling of particles, which manifests themselves in generating exotic low-energy scattering properties and significant many-body effects, as summarized below:

(A) The low-energy effective scattering will break SU(2) and SO(2) symmetries, i.e., the scattering process will no longer conserve any component of the total spin of incident particles.

(B) By tuning the rf field or magnetic field, all scattering channels will simultaneously go across the resonance, named as *multiple-channel scattering resonances* (MCSR).

(C) Near MCSR, a many-body system exhibits very different properties from those near a single-channel resonance. First, the spin-flip process is greatly enhanced, even in the presence of a weak rf field. Secondly, despite of the strong intra-species repulsion, the system exhibits evidently attractive correlations. These properties are experimentally detectable through the measurements of spin densities and two-body correlation functions.

The rest of the article is organized as follows. We set up the model Hamiltonian for our system in section II, and present the formula for solving the two-body problem in section III. The result of MCSR and its mechanism based on a two-channel model are discussed in section IV, and its many-body effect is studied in section V. Finally we summarize our results in section VI.

II. MODEL

We consider two-species bosons (denoted as \uparrow , \downarrow) in 1D geometry subject to tight transverse harmonic traps (with frequency ω_{\perp}) and a rf field (with strength Ω). The Hamiltonian for two such atoms located at $(\mathbf{r}_1, \mathbf{r}_2)$

is given by $H = \sum_{i=1}^2 H_i^{(0)} + U$, where

$$H_i^{(0)} = -\frac{\nabla_{x_i}^2 + \nabla_{y_i}^2}{2m} + \frac{m}{2}\omega_\perp^2(x_i^2 + y_i^2) + h_i^{(0)}, \quad (1)$$

$$U = \sum_{M=1,0,-1} U_{MM} \delta(\mathbf{r}_1 - \mathbf{r}_2) |M\rangle \langle M|. \quad (2)$$

Here

$$h_i^{(0)} = -\frac{\nabla_{z_i}^2}{2m} + \Omega \sigma_x^i \quad (3)$$

is the non-interacting hamiltonian along the 1D tube (z), and σ_x is Pauli matrix inducing spin-flip. U characterizes scattering in three channels classified by total magnetization M , and specifically

$$|M=1\rangle = |\uparrow_1 \uparrow_2\rangle, \quad (4)$$

$$|M=0\rangle = \frac{1}{\sqrt{2}}(|\uparrow_1 \downarrow_2\rangle + |\downarrow_1 \uparrow_2\rangle), \quad (5)$$

$$|M=-1\rangle = |\downarrow_1 \downarrow_2\rangle. \quad (6)$$

U in each M -channel is associated with a s-wave scattering length a_M , via

$$\frac{1}{U_{MM}} = \frac{4\pi a_M}{m} - \frac{1}{V} \sum_{\mathbf{k}} \frac{m}{k^2}, \quad (7)$$

where V is the volume.

To realize above model Hamiltonian, one can use $F=1$ alkali isotopes such as ^{87}Rb , with $|m_F=1(0)\rangle \equiv |\uparrow(\downarrow)\rangle$. Through a FR at $B_0 = 1007G$, the scattering length a_1 can be tuned efficiently (but not a_0, a_{-1}). At magnetic field $B \sim B_0$, the large Zeeman splitting between \uparrow and \downarrow spins can be effectively eliminated by applying a rf field and tuning its frequency on resonance with the splitting. In the frame rotating at the rf frequency, a spinor bosonic system (without Zeeman splitting due to external B) can be created. Similar setup has been realized in a previous experiment[23]. Note that the third component of $F=1$ isotopes, $|m_F=-1\rangle$, can be adiabatically eliminated due to the large quadratic Zeeman shift at $B \sim B_0$ [24].

For the low-energy scattering, we will show that the system can be described by an effective 1D Hamiltonian: $h = \sum_{i=1}^2 h_i^{(0)} + u$, with

$$u = \sum_{MN} u_{MN} \delta(z_1 - z_2) |M\rangle \langle N|. \quad (8)$$

Here u_{MN} is the effective 1D coupling strength between channel M and N , and we have expressed Eq.(8) in a most general form with off-magnetization scattering terms (i.e., u_{MN} with $M \neq N$). As we will show in this work, these terms do exist in u , hence demonstrating a unique scattering property of the confined 1D system in comparison with the 3D one (see U in Eq.(2)). In the following we will calculate u by matching the two-body solutions of H and h , with the only criterion that they produce the same low-energy scattering property.

III. TWO-BODY FORMULISM

We study the full scattering wavefunction $|\Psi\rangle$ according to $H|\Psi\rangle = E|\Psi\rangle$, with low energy $E \ll E_{th} + 2\omega_\perp$ where $E_{th} = \omega_\perp - 2\Omega$ is the threshold energy. We only consider the relative motion here since it is interaction-relevant and can be decoupled from the center-of-mass motion. Given U in (2), we assume

$$\langle \mathbf{r} | U | \Psi \rangle = \delta(\mathbf{r}) \sum_{M=-1,0,1} F_M |M\rangle, \quad \mathbf{r} \equiv \mathbf{r}_1 - \mathbf{r}_2 \quad (9)$$

Further utilizing the Lippman-Schwinger equation

$$U|\Psi\rangle = T|\Psi^{(0)}\rangle, \quad (10)$$

where the T-matrix follows

$$T = U + U G_0 T, \quad (11)$$

$|\Psi^{(0)}\rangle$ is the incident wave function and $G_0 = (E - H_1^{(0)} - H_2^{(0)} + i0^+)^{-1}$ is the non-interacting Green function, we obtain the scattering amplitudes $\{F_M\}$ in (9) via following matrix equation[25]

$$\sum_N \left[U^{-1} - \tilde{G}_0 \right]_{MN} F_N = \tilde{\Psi}_M^{(0)}; \quad (12)$$

with $\tilde{G}_0 = G_0(\mathbf{r} = \mathbf{0})$, $\tilde{\Psi}_M^{(0)} = \langle M | \Psi^{(0)}(\mathbf{r} = \mathbf{0}) \rangle$. Here U and \tilde{G}_0 are both 3×3 matrixes expanded in the $\{|M\rangle \langle N|\}$ spin basis. After solving $\{F_M\}$ from (12), we obtain the wave function as

$$\Psi(\mathbf{r}) = \Psi^{(0)}(\mathbf{r}) + \sum_M F_M G_0(\mathbf{r}) |M\rangle. \quad (13)$$

When $z \rightarrow \infty$, the wave function (13) is frozen at the lowest transverse mode ($n_x = n_y = 0$), i.e.,

$$\Psi(\mathbf{r}) \rightarrow \phi_0(x) \phi_0(y) \psi(z). \quad (14)$$

Here ψ describes the effective scattering process along z , which can be equally obtained based on the reduced 1D Hamiltonian h . Similarly we define the 1D scattering amplitudes f_M , and find that Eqs.(9,12) are still applicable as long as $\{z, \Psi, \Psi^{(0)}, F_M, U, G_0\}$ are respectively replaced by $\{z, \psi, \psi^{(0)}, f_M, u, g_0\}$, where $g_0 = (E - E_{th} - h_1^{(0)} - h_2^{(0)} + i0^+)^{-1}$ is non-interacting Green function in 1D. Given Eq.(14), we get $f_M = F_M \phi_0^{*2}(0)$ and finally relate u in (8) to U in (2) as

$$u = |\phi_0(0)|^4 [U^{-1} - \tilde{G}_0^{ex}]^{-1}, \quad \tilde{G}_0^{ex} = \tilde{G}_0 - |\phi_0(0)|^4 \tilde{g}_0 \quad (15)$$

Here \tilde{G}_0^{ex} is the Green function constructed by all excited transverse modes $n_x + n_y > 0$. As we will see later, its structure is essential to induce the multiple-channel scattering resonances in u . In Appendix A, we present more details for the derivation and evaluation of matrix equations (12) and (15).

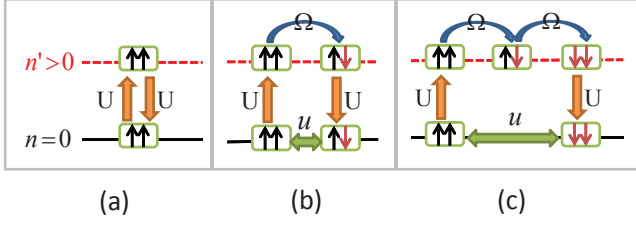


FIG. 1: (Color Online). Schematic plots of virtual scattering processes involving higher excited modes without (a) or with (b,c) rf field. u_{11} , u_{10} and $u_{1,-1}$ are respectively renormalized through the processes in (a), (b) and (c).

IV. MULTIPLE-CHANNEL SCATTERING RESONANCE (MCSR)

In this section, we present the result of multiple-channel scattering resonance for the reduced 1D coupling strengths, and analyze its physical mechanism based on a two-channel model, which provides a useful estimation on the resonance widths in different scattering channels.

A. Results

Cooperating with the confinement and 3D interactions, the rf field can result in multi-channel effective scattering in the low-energy 1D space. This is achieved through the virtual scattering processes to higher transverse modes, as schematically shown in Fig.1. Without rf field (Fig.1a), an initial spin state, $|\uparrow\uparrow\rangle (M=1)$, at the ground state mode ($\mathbf{n} : n_x = n_y = 0$), can only be scattered by 3D interaction U to the same spin state in higher modes ($\mathbf{n}' : n_x + n_y > 0$), and then back to itself in \mathbf{n} , which process renormalizes the effective u_{11} . When rf field is switched on, two additional processes can occur (Fig.1b and 1c). The rf field could flip spins in \mathbf{n}' once or twice and finally be scattered to a different spin state $|\uparrow\downarrow\rangle (M=0)$ or $|\downarrow\downarrow\rangle (M=-1)$ in the ground mode \mathbf{n} . These processes respectively renormalize u_{10} and $u_{1,-1}$, which are originally absent if without rf field.

More accurately, the physics illustrated above can be reflected in the exact expression of \tilde{G}_0^{ex} (Eq.(15)), which include both diagonal and off-diagonal elements contributed from all orders of scattering processes involving all excited modes. Consequently, u -matrix also have non-zero off-diagonal elements, which break both SU(2) and SO(2) symmetries in the spin-spin scattering process. This exactly demonstrates the multiple-channel scattering as summarized previously by (A) in the introduction.

Moreover, due to the intrinsic entanglement between different scattering processes, Eq.(15) further predicts an exotic phenomenon in the low-energy scattering, namely the *multiple-channel scattering resonances* (MCSR), which refers to a simultaneous divergence of effective couplings in different scattering channels (dif-

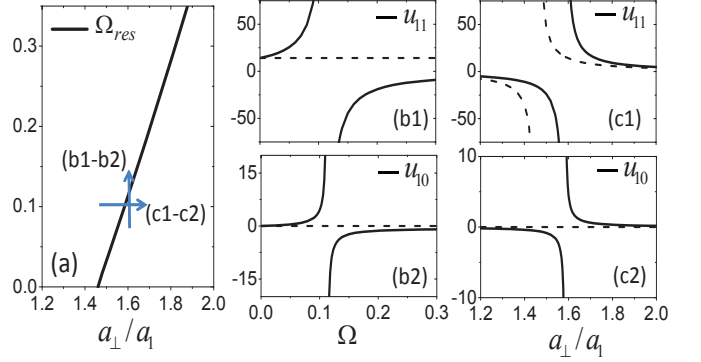


FIG. 2: (Color Online). Multiple-channel scattering resonances with tunable a_1 and fixed $a_0 = a_{-1} = a_{\perp}/4$ [24]. Ω is scaled by ω_{\perp} , and u_{11} , u_{10} are scaled by $2/(m\omega_{\perp})$. (a): Resonance position Ω_{res} as functions of a_{\perp}/a_1 . (b1,b2) [or (c1,c2)]: u_{11} , u_{10} as functions of Ω at fixed $a_{\perp}/a_1 = 1.6$ [or as functions of a_{\perp}/a_1 at fixed $\Omega = 0.1\omega_{\perp}$], corresponding to the blue vertical [or horizontal] arrow in (a). For comparison, CIR predictions[17] are shown by dashed lines.

ferent u -matrix elements). For threshold scattering ($E = E_{th}$), the MCSR occurs when

$$|U^{-1} - \tilde{G}_0^{ex}(E = E_{th}, \Omega_{res})| = 0. \quad (16)$$

Here Ω_{res} is the strength of rf field required by MCSR. Remarkably, it means that by tuning one single parameter (Ω or scattering length a_M in an arbitrary M -channel), the spinor system can be driven to strongly coupling regime in multiple scattering channels. This demonstrates (B) in the introduction. Note that the MCSR here should be distinguished from the coupled-channel scattering[26] and the multi-channel quantum defect theory[27] studied in literature[28].

In Fig.2, we show the general features of MCSR by numerically solving Eqs.(15,16). Fig.2(a) gives Ω_{res} as a function of one interaction parameter a_{\perp}/a_1 ($a_{\perp} = \sqrt{2/(m\omega_{\perp})}$ is confinement length), while a_0 and a_{-1} are both fixed and far off resonance. This resembles the actual case of ^{87}Rb in realistic experiments[24]. At $\Omega = 0$, different scattering channels are decoupled and we recover the result of CIR within the single $M = 1$ channel at $a_{\perp}/a_1 = 1.46$ [17]. At finite Ω , it is found that the resonance position shifts to BEC side with larger a_{\perp}/a_1 . More importantly, the structure of u is drastically different from what CIR predicted (dashed curves in Fig.2(b1,b2,c1,c2)). Especially, by tuning Ω we find non-zero off- M scattering u_{10} ($M = 1 \leftrightarrow M = 0$, Fig.2(b2)), with its strength approaching resonance regime simultaneously with u_{11} ($M = 1 \leftrightarrow M = 1$, Fig.2(b1)). These multiple resonances can also be achieved by tuning a_{\perp}/a_1 while keeping Ω fixed (Fig.2(c1,c2)).

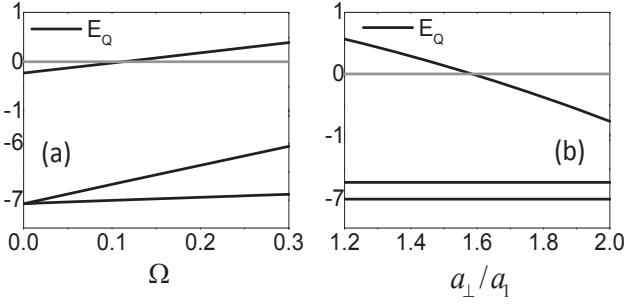


FIG. 3: Virtual bound state energies E_Q (shifted by E_{th}) as functions of Ω at fixed $a_{\perp}/a_1 = 1.6$ (a), or as functions of a_{\perp}/a_1 at fixed $\Omega = 0.1\omega_{\perp}$ (b). Here (a) and (b) respectively follow the vertical or horizontal arrows in Fig.2(a). E_Q , Ω are all scaled by ω_{\perp} .

B. Physical mechanism of MCSR

Following the traditional way in understanding FR[29] and CIR[17], a thorough physical interpretation for MCSR can also be obtained through a two-channel model, where an open channel and a closed channel are introduced respectively with projection operators P and Q . Here the open (P) channel refers to scattering within the lowest transverse mode ($n_x = n_y = 0$), while the closed (Q) channel refers to scattering involving higher transverse modes ($n_x + n_y > 0$). With projections P and Q , the two-body schrodinger equation can be divided into two equations,

$$H_{PP}\Psi_P + H_{PQ}\Psi_Q = E\Psi_P; \quad (17)$$

$$H_{QP}\Psi_P + H_{QQ}\Psi_Q = E\Psi_Q, \quad (18)$$

with $H_{\mu\nu} = \mu H \nu$ and $\Psi_{\mu} = \mu \Psi$ ($\mu, \nu = P$ or Q). By solving these equations, one can obtain the effective schrodinger equation for the open-channel state Ψ_P as $H_{eff}\Psi_P = E\Psi_P$, with effective Hamiltonian

$$H_{eff} = H_{PP} + H_{PQ} \frac{1}{E - H_{QQ}} H_{QP}. \quad (19)$$

The second term of above equation incorporates all contributions from the virtual scattering processes involving higher transverse modes (closed channel), which renormalize the effective scattering within the lowest transverse mode (open channel). As the eigen-value of H_{QQ} can be adjusted by interaction parameters or the strength of rf field, it can be tuned crosses E_{th} and cause a divergence of H_{eff} according to Eq.(19). This gives rise to the scattering resonance in the open channel.

We denote the eigen-states of H_{QQ} as $\tilde{\Psi}_Q$, and write $H_{QQ}\tilde{\Psi}_Q = E_Q\tilde{\Psi}_Q$. $E_Q = E_{th}$ determines the scattering resonances for open channel. In Fig.3, we plot three E_Q evolving with the rf strength or interaction parameters, and the place when one of these bound states across E_{th} gives the location of MCSR. Different from the closed-channel bound state in a single-channel resonance, here

in MCSR each bound state is highly entangled in spin space, which is a certain superposition of all M -states. Whenever such a dressed-spin state across threshold, resonances will simultaneously occur in multiple spin-collision channels, as seen from Fig.2(b1,b2,c1,c2).

Using the formula in Eq.(19), one can evaluate the resonance width in different collision channels, which is proportional to $H_{PQ}H_{PQ} = \langle \Psi_P | H | \tilde{\Psi}_Q \rangle \langle \tilde{\Psi}_Q | H | \Psi_P \rangle$. Explicitly, in our case we write the a_1 -tuned resonances as

$$u_{MN} = \frac{W_{MN}}{a_{\perp}/a_1 - C}, \quad (20)$$

$$W_{MN} \propto \langle \Psi_P^M | H | \tilde{\Psi}_Q \rangle \langle \tilde{\Psi}_Q | H | \Psi_P^N \rangle, \quad (21)$$

where C the resonance position of a_{\perp}/a_1 , $|\Psi_P^N\rangle$ is the open-channel wave function when projected to $|N\rangle$ spin state, and W_{MN} the resonance width of u_{MN} .

Given that a_1 can be tuned large through FR, while a_0 and a_{-1} are far off resonances (small positive values), in the vicinity of above 1D resonances the closed channel is mainly composed by $|M = 1\rangle$ states, and its wave function can be estimated through the perturbation theory, i.e.,

$$\begin{aligned} \tilde{\Psi}_Q(\mathbf{r}) = & \tilde{\Psi}_1^{(0)}(\mathbf{r})|M=1\rangle + \tilde{\Psi}_0^{(0)}(\mathbf{r}) \frac{\sqrt{2}\Omega \langle \tilde{\Psi}_0^{(0)} | \tilde{\Psi}_1^{(0)} \rangle}{E_1^{(0)} - E_0^{(0)}} |M=0\rangle \\ & + \tilde{\Psi}_{-1}^{(0)}(\mathbf{r}) \frac{2\Omega^2 \langle \tilde{\Psi}_{-1}^{(0)} | \tilde{\Psi}_0^{(0)} \rangle \langle \tilde{\Psi}_0^{(0)} | \tilde{\Psi}_1^{(0)} \rangle}{(E_1^{(0)} - E_0^{(0)})(E_1^{(0)} - E_{-1}^{(0)})} |M=-1\rangle \end{aligned} \quad (22)$$

here $\tilde{\Psi}_M^{(0)}(\mathbf{r})$ and $E_M^{(0)}$ are respectively the eigen-function and eigen-energy of H_{QQ} in $M \leftrightarrow M$ scattering channel at $\Omega = 0$. Given above interaction parameters, we have $E_1^{(0)} \gg E_0^{(0)} = E_{-1}^{(0)} \approx -1/(ma_0^2)$ or $\approx -1/(ma_{-1}^2)$. Above perturbation theory is valid when

$$\frac{\Omega}{|E_1^{(0)} - E_{0(-1)}^{(0)}|} \ll 1. \quad (23)$$

Given Eq.(21) and Eq.(22), one can obtain the relative widths of all $\{W_{MN}\}$. For instance, we have the ratios

$$\frac{W_{10}}{W_{11}} \sim \frac{\Omega}{E_1^{(0)} - E_0^{(0)}}; \quad (24)$$

$$\frac{W_{00}}{W_{11}} \sim \frac{\Omega^2}{(E_1^{(0)} - E_0^{(0)})^2}; \quad (25)$$

$$\frac{W_{1,-1}}{W_{11}} \sim \frac{\Omega^2}{(E_1^{(0)} - E_0^{(0)})(E_1^{(0)} - E_{-1}^{(0)})}, \quad (26)$$

From this estimation, one can see that under the condition (23), only W_{11} and W_{10} would have visible widths, while the others (in comparison to W_{11} and W_{10}) are too narrow to be resolve in realistic experiments.

Above analyses from two-channel model have also been verified by our numerical calculations. Fig.4 shows that all the elements of u -matrix simultaneously go to infinity

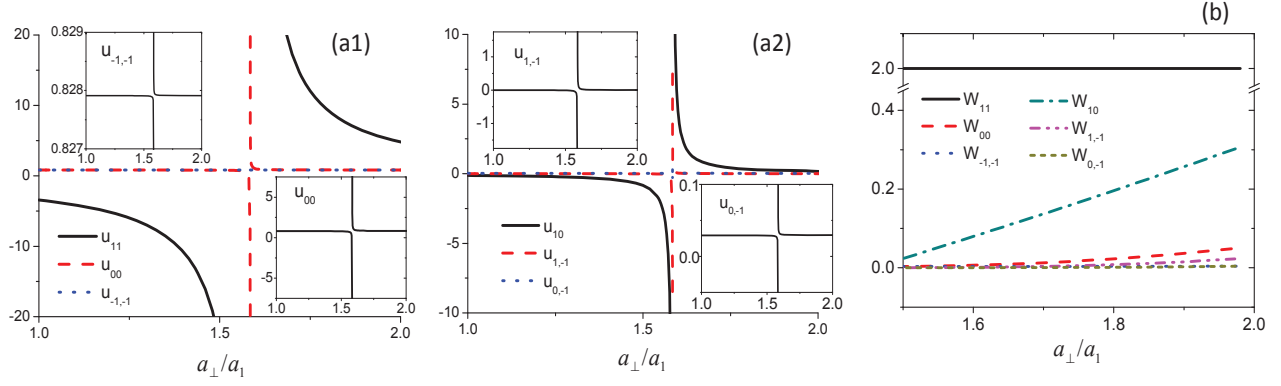


FIG. 4: (Color Online). (a1) Diagonal and (a2) off-diagonal matrix elements of u as functions of a_{\perp}/a_1 at fixed $\Omega = 0.1\omega_{\perp}$. The other parameters, $a_0 = a_{-1} = a_{\perp}/4$, are the same as those in Fig.2. Insets show magnified plots of u -matrix elements except for u_{11} and u_{10} . (b) Resonance widths W_{MN} defined in Eq.(21). u -elements and W_{MN} are both scaled by $2/(m\omega_{\perp})$.

as a_{\perp}/a_1 across resonance position. However, under the conditions specified before Eq. (22), only the resonances of u_{11} and u_{10} have visible widths. The other components of u -matrix are only large enough if extremely close to

the resonance position (with very narrow width). In the following, we will explore the many-body effect due to strong couplings of u_{11} and u_{10} near MCSR, while the other channels are approximated as non-interacting.

V. MANY-BODY EFFECTS

Given u_{11} and u_{10} from two-body solutions, we write down the many-body Hamiltonian for 1D spinor bosons subject to an additional harmonic trap,

$$\begin{aligned}
 H = & \sum_{\sigma} \int dz \Psi_{\sigma}^{\dagger}(z) \left(-\frac{\hbar^2}{2m} \frac{\partial^2}{\partial z^2} + \frac{1}{2} m \omega_T z^2 \right) \Psi_{\sigma}(z) \\
 & + \Omega \int dz \left(\Psi_{\uparrow}^{\dagger}(z) \Psi_{\downarrow}(z) + h.c. \right) \\
 & + \frac{u_{11}}{2} \int dz \Psi_{\uparrow}^{\dagger}(z) \Psi_{\uparrow}^{\dagger}(z) \Psi_{\uparrow}(z) \Psi_{\uparrow}(z) \\
 & + \frac{u_{10}}{\sqrt{2}} \int dz \left(\Psi_{\uparrow}^{\dagger}(z) \Psi_{\uparrow}^{\dagger}(z) \Psi_{\uparrow}(z) \Psi_{\downarrow}(z) + h.c. \right) \quad (27)
 \end{aligned}$$

It is clear that the interaction part of H includes various terms breaking $SU(2)$ and $SO(2)$ symmetries, such as $\rho \cdot \sigma_z$, $\rho \cdot \sigma_x$, $\sigma_z \cdot \sigma_z$, $\sigma_z \cdot \sigma_x$, where ρ and $\sigma_{x,z}$ are respectively the number density and spin densities.

Based on Hamiltonian (10), we will first use exact diagonalization method to solve the ground state of a four-particle system. The results obtained not only are relevant to the cluster system[30, 31], but also serve as a benchmark for a many-body system. We focus on the large repulsion limit of u_{11} , where u_{10} can also be tuned large and positive using MCSR. To highlight the significance of u_{10} , we compare three different cases: (i) strongly repulsive spin- \uparrow bosons without rf field ($\Omega = 0$) and $u_{10} = 0$; (ii) $\Omega \neq 0$ but still $u_{10} = 0$; (iii) $\Omega \neq 0$ and $u_{10} \neq 0$. Among them, case (iii) is what we are most

interested in and also the general one near MCSR.

In Fig.5 we show the spin density distributions,

$$\rho_{\sigma}(z) \equiv \langle \Psi_{\sigma}^{\dagger}(z) \Psi_{\sigma}(z) \rangle, \quad (28)$$

and the two-body correlation functions,

$$g_{\sigma\sigma'}(z, z_0) \equiv \langle \Psi_{\sigma}^{\dagger}(z) \Psi_{\sigma'}^{\dagger}(z_0) \Psi_{\sigma'}(z_0) \Psi_{\sigma}(z) \rangle \quad (29)$$

with $z_0 = 0$, for $N = 4$ system in cases (i,ii,iii). For case (i), the spin- \uparrow bosons are fermionalized, with wave function well approximated by the absolute value of a Slater determinant $\psi_{\uparrow}(\{z\}) = \sqrt{\frac{1}{N!}} |Det(\phi_i(z_j))|$ (here ϕ_i is the eigen-function of 1D harmonic oscillator, with level index $i = 0, \dots, N-1$). Consequently the density is given by $\rho_{\uparrow}(z) = \sum_{i=0}^{N-1} |\phi_i(z)|^2$, and the two-body correlation by $g_{\uparrow\uparrow}(z, z_0) = \sum_{\langle i,j \rangle} |\phi_i(z) \phi_j(z_0) - \phi_j(z) \phi_i(z_0)|^2$, which all share the same properties of identical fermions (see gray curves in Fig.5(a1,b1)). When turn on a weak rf, it provides a way to avoid strong repulsion between \uparrow -spins by flipping them to \downarrow , and thus the ground state will be tremendously changed[32]. If u_{10} is absent(case (ii)), rf alone will generate a lot more \downarrow than \uparrow (see Fig.5(a2)). The residual \uparrow are there to take advantage of the rf energy, and they still maintain fermion-like correlations, characterized by a dip of $g_{\uparrow\uparrow}$ at $z = z_0 = 0$ (Fig.5(b2)).

Compared with cases (i,ii) which describe a single-channel resonance, the case (iii), with u_{10} present and describing MCSR, will show a very different ground state property (as summarized by (C)). As the u_{10} term follows the form of $\int dz \rho_{\uparrow}(z) \sigma_x(z)$, the spin-flip process

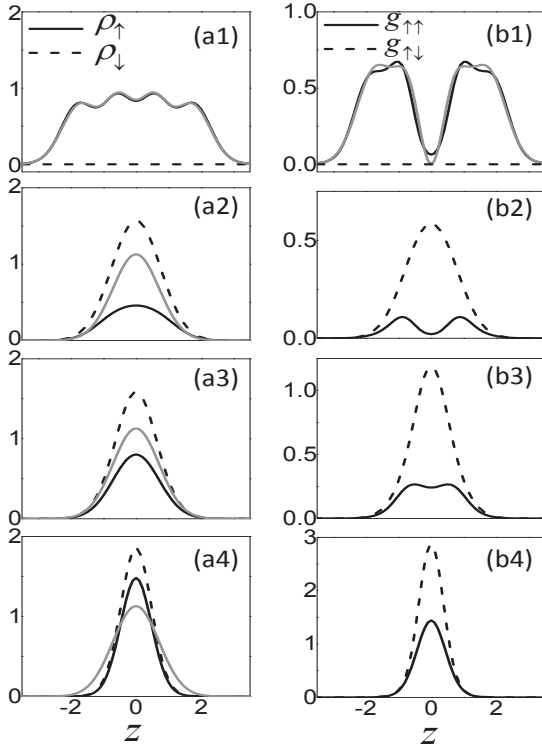


FIG. 5: (Color Online). (a1-a4) Spin densities (in units of $1/a_T$, $a_T = (m\omega_T)^{-1/2}$) and (b1-b4) correlation functions (in units of $1/a_T^2$) for four trapped bosons in 1D. z is in unit of a_T . The parameters, $(u_{11}/(a_T\omega_T), u_{10}/(a_T\omega_T), \Omega/\omega_T)$, are respectively: (a1,b1)(12, 0, 0); (a2,b2)(12, 0, 1); (a3,b3)(12, $2\sqrt{2}$, 1); (a4,b4)(12, $4\sqrt{2}$, 1). For comparison, gray curves in (a1,b1) show the case of identical fermions (see text), and in (a2-a4) show the density distribution of non-interacting bosons.

will be drastically enhanced through u_{10} . As shown in Fig.5(a3) and (a4), the spin numbers get more balanced as u_{10} increases. One may thus expect this u_{10} term just simply enhance the effective rf strength, Ω_{eff} . However, this is not true, as it also generates significant interac-

tion effect and modifies the pair correlations. As seen from Fig.5(b3) and (b4), when increasing u_{10} from zero, the original dip of up-spin correlations at $z = z_0 = 0$ gradually vanishes and turns to a peak, implying the up-spins gradually lose their repulsive nature and turn attractive. Accordingly all spins are attracted to the trap center and produce more pronounced density distribution (than non-interacting case)(Fig.2(a4)). Indeed, assume a many-body system at sufficiently large u_{10} , one would expect the spins being polarized along $-\hat{x}$, giving $\sigma_x(z) = -2\rho_\downarrow(z) = -2\rho_\uparrow(z)$. Eventually the total interaction becomes $\frac{1}{8}(u_{11} - 2\sqrt{2}u_{10}) \int dz \rho^2(z)$, which becomes purely attractive if $u_{10} \gg u_c \equiv u_{11}/(2\sqrt{2})$ [33].

VI. SUMMARY

In summary, we have demonstrated that a multiple-channel scattering resonance(MCSR) can be achieved for spinor bosons confined in 1D geometry. The two-body and many-body properties revealed in this work are expected to be easily probed in current cold atoms experiments.

Finally, we remark that the proposal of MCSR widely applies to other high-spin systems which allow more-than-one collision channels, and other confined geometries such as 2D. Moreover, rf field can be replaced by any field that allows spin-flips, such as a rotating magnetic field generating spin-orbit couplings[34]. Given the wide applicability and special properties of MCSR, we expect this new type of scattering resonance will induce a lot more intriguing many-body physics in the subject of spinor systems, such as the ground state structure and topological defects of a 2D BEC, the pairing superfluidity of high-spin fermions, the interplay effect with spin-orbit correlations and so on.

The author thanks Randy Hulet, Shuai Chen, Hui Zhai, Tin-Lun Ho, Xi-Wen Guan and Jian Li for stimulating discussions, and Wenbo Fu for early contribution on this project. This work is supported by NSFC under Grant No. 11104158, No. 11374177, and programs of Chinese Academy of Sciences.

Appendix A: Derivation of u -matrix (Eq.(15))

First, we decouple the non-interacting two-body Hamiltonian as follows,

$$H_1^{(0)} + H_2^{(0)} = \left(-\frac{\nabla_X^2 + \nabla_Y^2 + \nabla_Z^2}{4m} + m\omega_\perp^2(X^2 + Y^2) \right) + \left(-\frac{\nabla_x^2 + \nabla_y^2 + \nabla_z^2}{m} + \frac{m}{4}\omega_\perp^2(x^2 + y^2) + \Omega(\sigma_x^1 + \sigma_x^2) \right) \quad (\text{A1})$$

Here the first bracket represents the Hamiltonian for center-of-mass motion $\mathbf{R} \equiv (X, Y, Z) = \frac{\mathbf{r}_1 + \mathbf{r}_2}{2}$ with effective mass $2m$; the second bracket includes the relative motion $\mathbf{r} \equiv (x, y, z) = \mathbf{r}_1 - \mathbf{r}_2$ with mass $m/2$, and the spin part according to a transverse magnetic field. Since the interaction U is only relevant to the relative motion and their spins, we only consider the second bracket in Eq.(A1) when solving two-body problem in the following.

The eigen-state for non-interacting Hamiltonian (second bracket in Eq.(A1)) can be expressed as $|n_x, n_y, k\rangle|\alpha_1\beta_2\rangle$,

where the first part describes the relative motion with wave function

$$\langle x, y, z | n_x, n_y, k \rangle = \phi_{n_x}(x) \phi_{n_y}(y) \frac{e^{ikz}}{\sqrt{L_z}}, \quad (\text{A2})$$

and the second part shows the spin configuration with $\alpha, \beta = +$ or $-$, and $|\pm\rangle = (|\uparrow\rangle \pm |\downarrow\rangle)/\sqrt{2}$. The corresponding energy spectrum is

$$E_{n_x, n_y, k; \alpha_1 \beta_2} = (n_x + n_y + 1)\omega_\perp + \frac{k^2}{m} + (\epsilon_\alpha + \epsilon_\beta), \quad (\text{A3})$$

here $\epsilon_\pm = \pm\Omega$. The threshold scattering energy is therefore $E_{th} = \omega_\perp - 2\Omega$ when $n_x = n_y = 0$, $k = 0$, $\alpha = \beta = -$.

Making use of the Lippman-Schwinger equation $U|\Psi\rangle = T|\Psi^{(0)}\rangle$, and the T-matrix $T = U + UG_0T$, we get

$$U|\Psi\rangle = U|\Psi^{(0)}\rangle + UGU|\Psi\rangle, \quad (\text{A4})$$

then combining with Eq.(9) in the text, we obtain the matrix equation expanded in $\{|M\rangle\langle N|\}$ spin space, (see also Eq.(12) in the text)

$$\left[\begin{pmatrix} U \end{pmatrix}^{-1} - \begin{pmatrix} \tilde{G}_0 \equiv G_0(\mathbf{r} = \mathbf{0}) \end{pmatrix} \right] \begin{pmatrix} F_1 \\ F_0 \\ F_{-1} \end{pmatrix} = \begin{pmatrix} \tilde{\Psi}_1^{(0)} \\ \tilde{\Psi}_0^{(0)} \\ \tilde{\Psi}_{-1}^{(0)} \end{pmatrix}, \quad (\text{A5})$$

here matrix $(U) = \text{diag}(U_1, U_0, U_{-1})$; $[\tilde{G}_0(\mathbf{r})]_{MN} = \langle \mathbf{r}, M | G_0 | \mathbf{0}, N \rangle$; $\tilde{\Psi}_M^{(0)} = \langle M | \Psi^{(0)}(\mathbf{r} = \mathbf{0}) \rangle$. With the information of F_M from above matrix equation, the wf can be deduced straightforwardly, which is Eq.(13) in the text.

For low-energy scattering $E \ll E_{th} + 2\omega_\perp$ and at $z \rightarrow \infty$, in the full wave function all excited \mathbf{n} (with $n_x + n_y > 0$) modes decays away except the lowest \mathbf{n}_0 ($n_x = n_y = 0$), i.e., the wave function is effectively propagating in 1D as

$$\Psi(\mathbf{r}) \rightarrow \phi_0(x)\phi_0(y) \left\{ \psi^{(0)}(z) + g_0(z)(f_1|1\rangle + f_0|0\rangle + f_{-1}|-1\rangle) \right\} \quad (\text{A6})$$

with $f_M = F_M \phi_0^{*2}(0)$, and g_0 is the non-interacting Green function for 1D system (see definition in the text). Alternatively, the wave function along z can be generated effectively through a 1D interaction

$$\langle z | u | \psi \rangle = \delta(z)(f_1|1\rangle + f_0|0\rangle + f_{-1}|-1\rangle), \quad (\text{A7})$$

together with the Lippman-Schwinger equation

$$\left[\begin{pmatrix} u \end{pmatrix}^{-1} - \begin{pmatrix} \tilde{g}_0 \equiv g_0(z = 0) \end{pmatrix} \right] \begin{pmatrix} f_1 \\ f_0 \\ f_{-1} \end{pmatrix} = \begin{pmatrix} \tilde{\psi}_1^{(0)} \\ \tilde{\psi}_0^{(0)} \\ \tilde{\psi}_{-1}^{(0)} \end{pmatrix}. \quad (\text{A8})$$

Compare Eq.(A8) with Eq.(A5), and recall the relations that $f_M = F_M \phi_0^{*2}(0)$, $\tilde{\psi}_M^{(0)} = \tilde{\Psi}_M^{(0)}/\phi_0^2(0)$, we obtain

$$\begin{pmatrix} u \end{pmatrix}^{-1} - \begin{pmatrix} \tilde{g}_0 \end{pmatrix} = \frac{1}{|\phi(0)|^4} \left[\begin{pmatrix} U \end{pmatrix}^{-1} - \begin{pmatrix} \tilde{G}_0 \end{pmatrix} \right], \quad (\text{A9})$$

which gives rise to Eq.(15) in the text.

Next we show the detailed procedure how to evaluate \tilde{G}_0^{ex} and u -matrix in Eq.(8). To expand \tilde{G}_0^{ex} , one needs to insert a complete set of eigen-states $\{|n_x, n_y, k\rangle|\alpha_1\beta_2\rangle\}$ and sum over all contributions from these energy states. We will see in the following that for a diagonal element of \tilde{G}_0^{ex} , the summation will have ultraviolet divergence, which will be compensated by the same divergence in U^{-1} . Eventually each element of u is physically a finite value.

As the ultraviolet divergence in energy space corresponds to the short-range singularity of the wave function ($\sim 1/r$) as inter-particle distance $r \rightarrow 0$, in the following we will try to exact the physical value of \tilde{G}_0^{ex} by evaluating the Green function in coordinate space and subtracting $1/r$ singularities. Explicitly, take one diagonal element ($M = N = 1$) of example, we have

$$\begin{aligned} [G_0^{ex}(\mathbf{r})]_{11} &= \langle \mathbf{r}; M = 1 | G_0^{ex} | \mathbf{0}; M = 1 \rangle \\ &= \sum_{n_1+n_2>0}^{\infty} \phi_{n_1}(x) \phi_{n_1}^*(0) \phi_{n_2}(y) \phi_{n_2}^*(0) \int_{-\infty}^{\infty} \frac{dk}{2\pi} e^{ikz} \left(\sum_{\alpha, \beta} \frac{\langle M = 1 | \alpha_1 \beta_2 \rangle \langle \alpha_1 \beta_2 | M = 1 \rangle}{\Delta E - (n_1 + n_2)\omega_\perp - \frac{k^2}{m} - (\epsilon_\alpha + \epsilon_\beta + 2\Omega) + i\delta} \right) \end{aligned} \quad (\text{A10})$$

with $\Delta E = E - E_{th}$; $\langle M = 1 | \alpha_1 \beta_2 \rangle = \xi_\alpha^\dagger \xi_\beta^\dagger$ and $\xi_\alpha^\dagger = \xi_\beta^\dagger = 1/\sqrt{2}$. Note that in order for the non-zero value of above equation as $\mathbf{r} \rightarrow 0$, $n_x + n_y$ should be an even integer ($= 2, 4, \dots$), therefore as long as $\Delta E < 2\omega_\perp$ the denominator inside the bracket is always negative. For this low-energy scattering ($\Delta E \ll 2\omega_\perp$), Eq.(A10) is transformed to

$$-\sum_{\alpha,\beta} |\langle M = 1 | \alpha_1 \beta_2 \rangle|^2 \int_0^\infty dt A(t) e^{(\Delta E)t} e^{-(\epsilon_\alpha + \epsilon_\beta + 2\Omega)t} \int_{-\infty}^\infty \frac{dk}{2\pi} e^{ikz} e^{-\frac{k^2}{m}t}, \quad (\text{A11})$$

and $A(t)$ can be obtained by making use of the propagator of 1D harmonic oscillator,

$$\begin{aligned} A(t) &= \left(\sum_{n_1=0}^\infty e^{-n_1\omega_\perp t} \phi_{n_1}(x) \phi_{n_1}^*(0) \right) \left(\sum_{n_2=0}^\infty e^{-n_2\omega_\perp t} \phi_{n_2}(y) \phi_{n_2}^*(0) \right) - \phi_0(x) \phi_0^*(0) \phi_0(y) \phi_0^*(0) \\ &= \frac{1}{\pi a_\perp^2} \left(\frac{1}{1 - e^{-2\omega_\perp t}} e^{-\frac{x^2+y^2}{2a_\perp^2} \coth(\omega_\perp t)} - e^{-\frac{x^2+y^2}{2a_\perp^2}} \right). \quad (a_\perp = \sqrt{\frac{2}{m\omega_\perp}}) \end{aligned} \quad (\text{A12})$$

Further using the identity

$$\int_{-\infty}^\infty \frac{dk}{2\pi} e^{ikz} e^{-\frac{k^2}{m}t} = \frac{1}{a_\perp \sqrt{2\pi\tau}} e^{-\frac{z^2}{2a_\perp^2\tau}}, \quad (\tau = \omega_\perp t) \quad (\text{A13})$$

Eq.(A11) is further reduced to

$$-\sum_{\alpha,\beta} |\langle M = 1 | \alpha_1 \beta_2 \rangle|^2 \frac{m}{(2\pi)^{3/2} a_\perp} \int_0^\infty \frac{d\tau}{\sqrt{\tau}} e^{\frac{\Delta E}{\omega_\perp} \tau} e^{-\frac{\epsilon_\alpha + \epsilon_\beta + 2\Omega}{\omega_\perp} \tau} \left(\frac{1}{1 - e^{-2\tau}} e^{-\frac{x^2+y^2}{2a_\perp^2} \coth \tau} - e^{-\frac{x^2+y^2}{2a_\perp^2}} \right) e^{-\frac{z^2}{2a_\perp^2\tau}}. \quad (\text{A14})$$

It is then noticed this integral has singularity at $\tau \rightarrow 0$ and as $r = \sqrt{x^2 + y^2 + z^2} \rightarrow 0$, and the singularity is given by

$$-\frac{m}{(2\pi)^{3/2} a_\perp} \int_0^\infty \frac{d\tau}{2\tau^{3/2}} e^{-\frac{r^2}{2a_\perp^2\tau}} = -\frac{m}{4\pi r}. \quad (\text{A15})$$

Apart from the singularity term, the (physical) constant term in the asymptotic form

$$\lim_{r \rightarrow 0} G_0^{ex}(\mathbf{r})_{11} = -\frac{m}{4\pi r} + C_{11} \quad (\text{A16})$$

can be extracted as

$$C_{11} = -\sum_{\alpha,\beta} |\langle M = 1 | \alpha_1 \beta_2 \rangle|^2 \frac{m}{(2\pi)^{3/2} a_\perp} \int_0^\infty \frac{d\tau}{\sqrt{\tau}} \left(e^{\frac{\Delta E}{\omega_\perp} \tau} e^{-\frac{\epsilon_\alpha + \epsilon_\beta + 2\Omega}{\omega_\perp} \tau} \left(\frac{1}{1 - e^{-2\tau}} - 1 \right) - \frac{1}{2\tau} \right). \quad (\text{A17})$$

Recalling that $\frac{1}{U_{11}} = \frac{m}{4\pi a_1} - \frac{1}{V} \sum_{\mathbf{k}} \frac{1}{(k^2/m)} = \frac{m}{4\pi a_1} - \lim_{r \rightarrow 0} \frac{m}{4\pi r}$, and combining with Eq.(A16), we get the element

$$[U^{-1} - \tilde{G}_0^{ex}]_{11} = \frac{m}{4\pi a_1} - C_{11}. \quad (\text{A18})$$

Similarly one can obtain diagonal C_{MM} for $M = 0, -1$, by replacing $M = 1$ with $M = 0, -1$ in Eq.(A17). The one-dimensional integration in term of imaginary time τ can be performed straightforwardly by numerics. In the case of $\Omega = 0$, we have $C_{MM} = \frac{m}{4\pi a_\perp} c_0$ that are identical for all M , with $c_0 = 1.46$ obtained previously for conventional CIR(see Ref.[2]).

The same strategy can be used to calculate off-diagonal elements of matrix $(U^{-1} - \tilde{G}_0^{ex})$, and one can find that the divergence of these elements at short distance will be absent. Explicitly we have ($M \neq N$)

$$C_{MN} = -\sum_{\alpha,\beta} \langle M | \alpha_1 \beta_2 \rangle \langle \alpha_1 \beta_2 | N \rangle \frac{m}{(2\pi)^{3/2} a_\perp} \int_0^\infty \frac{d\tau}{\sqrt{\tau}} e^{\frac{\Delta E}{\omega_\perp} \tau} e^{-\frac{\epsilon_\alpha + \epsilon_\beta + 2\Omega}{\omega_\perp} \tau} \left(\frac{1}{1 - e^{-2\tau}} - 1 \right); \quad (\text{A19})$$

$$[U^{-1} - \tilde{G}_0^{ex}]_{MN} = -C_{MN} \quad (\text{A20})$$

Knowing all the elements of matrix $(U^{-1} - \tilde{G}_0^{ex})$, the u -matrix can be obtained through Eq.(15).

- 80**, 885 (2008).
- [3] X.-W. Guan, M. T. Batchelor, C. Lee, *Rev. Mod. Phys.* **85**, 1633 (2013).
- [4] T. -L. Ho, *Phys. Rev. Lett.* **81**, 742 (1998).
- [5] T. Ohmi and K. Machinda, *J. Phys. Soc. Jpn.* **67**, 1822 (1998).
- [6] J. Stenger, S. Inouye, D. M. Stamper-Kurn, H. J. Miesner, A. P. Chikkatur and W. Ketterle, *Nature (London)* **396**, 345 (1998).
- [7] C. V. Ciobanu, S.-K. Yip, and Tin-Lun Ho, *Phys. Rev. A*, **61**, 033607 (2000).
- [8] M. Koashi and M. Ueda, *Phys. Rev. Lett.* **84**, 1066 (2000).
- [9] H. Pu, C. K. Law, S. Raghavan, J. H. Eberly, and N. P. Bigelow, *Phys. Rev. A* **60**, 1463 (1999).
- [10] M.-S. Chang, C. D. Hamley, M. D. Barrett, J. A. Sauer, K. M. Fortier, W. Zhang, L. You, and M. S. Chapman, *Phys. Rev. Lett.* **92**, 140403 (2004).
- [11] M.-S. Chang, Q. Qin, W. Zhang, L. You and M. S. Chapman, *Nat. Phys.* **1**, 111(2005).
- [12] A. Widera, F. Gerbier, S. Fölling, T. Gericke, O. Mandel, and I. Bloch, *Phys. Rev. Lett.* **95**, 190405 (2005).
- [13] H. Schmaljohann, M. Erhard, J. Kronjager, M. Kottke, S. van Staa, L. Cacciapuoti, J. J. Arlt, K. Bongs, and K. Sengstock, *Phys. Rev. Lett.* **92**, 040402 (2004).
- [14] J. S. Krauser, J. Heinze, N. Fläschner, S. Götze, O. Jürgensen, D.-S. Lühmann, C. Becker and K. Sengstock, *Nat. Phys.* **8**, 813 (2012).
- [15] F. Deuretzbacher, K. Fredenhagen, D. Becker, K. Bongs, K. Sengstock, and D. Pfannkuche, *Phys. Rev. Lett.* **100**, 160405 (2008). Nearly spin-independent interaction is considered there.
- [16] C. Chin, R. Grimm, P. Julienne and E. Tiesinga, *Rev. Mod. Phys.* **82**, 1225 (2010).
- [17] M. Olshanii, *Phys. Rev. Lett.* **81**, 938 (1998); T. Bergeman, M. G. Moore and M. Olshanii, *Phys. Rev. Lett.* **91**, 163201 (2003).
- [18] D. S. Petrov, M. Holzmann, and G. V. Shlyapnikov, *Phys. Rev. Lett.* **84**, 2551 (2000); D. S. Petrov and G. V. Shlyapnikov, *Phys. Rev. A* **64**, 012706 (2001).
- [19] T. Kinoshita, T. Wenger, and D.S. Weiss, *Science* **305**, 1125 (2004).
- [20] E. Haller, M. Gustavsson, M. J. Mark, J. G. Danzl, R. Hart, G. Pupillo, and H.-C. Nägerl, *Science* **325**, 1224 (2009).
- [21] B. Fröhlich, M. Feld, E. Vogt, M. Koschorreck, W. Zwerger, and M. Köhl, *Phys. Rev. Lett.* **106**, 105301 (2011).
- [22] E. Haller, M. Rabie, M.J. Mark, J.G. Danzl, R. Hart, K. Lauber, G. Pupillo, and H.-C. Nägerl, *Phys. Rev. Lett.* **107**, 230404 (2011).
- [23] K. Jiménez-García, L. J. LeBlanc, R. A. Williams, M. C. Beeler, A. R. Perry, I. B. Spielman, *Phys. Rev. Lett.* **108**, 225303 (2012).
- [24] For $F = 1$ ^{87}Rb the background scattering lengths are $a_1 \approx a_0 \approx a_{-1} = 5.3\text{nm}$. a_1 can be tuned through a FR at $B = 1007\text{G}$ [16]. Transverse confinement frequency is chosen to be $\omega_{\perp} = (2\pi)400\text{KHZ}$, giving confinement length $a_{\perp} = 24\text{nm}$. This gives $a_{\perp}/a_0 \approx a_{\perp}/a_{-1} \approx 4$, and a_{\perp}/a_1 is highly tunable. Near FR of a_1 , the Zeeman splitting between $m_F = 1$ and $m_F = 0$ is 0.63GHZ , while between $m_F = 0$ and $m_F = -1$ is 0.77GHZ due to the large quadratic Zeeman shift. Thus $m_F = -1$ can be adiabatically eliminated if the rf frequency matches 0.63GHZ . Similar adiabatic elimination of the third state in $F = 1$ systems has been achieved in previous experiments, see for example: Y.-J. Lin, K. Jiménez-García and I. B. Spielman, *Nature* **471**, 83 (2011).
- [25] X. Cui, *Few-Body Syst.*, **52**, 65 (2012).
- [26] F. H. Mies, E. Tiesinga, and P. S. Julienne, *Phys. Rev. A* **61**, 022721(2000); J. M. Hutson, E. Tiesinga, and P. S. Julienne, *Phys. Rev. A* **78**, 052703(2008).
- [27] J. F. E. Croft, A. O. G. Wallis, J. M. Hutson, and P. S. Julienne, *Phys. Rev. A* **84**, 042703 (2011); Z. Idziaszek, T. Calarco, P. S. Julienne, A. Simoni, *Phys. Rev. A* **79**, 010702 (2009).
- [28] The "mixed-channel scattering" in Ref.[26] and [27] refers to scattering between different orbital angular momenta, which is due to the interplay effect of short-range interparticle interaction, the magnetic dipole interaction, the fine and hyperfine coupling, and the magnetic Zeeman energy. While the "multiple-channel" in our work refers to scattering between different total spin magnetizations, due to the interplay of the s-wave interaction, the confinement and the spin-flipping field. As a result, their physical consequences are also substantially different.
- [29] S. J. J. M. F. Kokkelmans, J. N. Milstein, M. L. Chiofalo, R. Walser, and M. J. Holland, *Phys. Rev. A* **65**, 053617 (2002).
- [30] F. Serwane, G. Zürn, T. Lompe, T. B. Ottenstein, A. N. Wenz, S. Jochim, *Science* **332**, 336 (2011).
- [31] G. Zürn, F. Serwane, T. Lompe, A. N. Wenz, M. G. Ries, J. E. Bohn, S. Jochim, *Phys. Rev. Lett.* **108**, 075303 (2012).
- [32] To avoid the system being polarized by rf field, we consider $\Omega \ll E_F$, where E_F is the Fermi energy of identical fermions with the same density as bosons.
- [33] The ratio of u_{10} to u_{11} near MCSR is directly given by the ratio of their individual width, which is tunable through the rf strength and interaction parameters. For a weak rf field, this ratio cannot be too large, so the system will hardly be fully polarized or turn purely attractive.
- [34] See a recent review by V. Galitski and I. B. Spielman, *Nature* **494**, 49 (2013).